

# Radiation efficiencies of the pulsars detected in the optical range

Zharikov S.<sup>a</sup>, Shibarov Yu.<sup>b</sup>, Komarova V.<sup>c</sup>

<sup>a</sup>OAN IA UNAM, Ensenada, BC, Mexico

<sup>b</sup>Ioffe Physical Technical Inst, RAS, St. Petersburg, Russia

<sup>c</sup>Special Astrophysical Observatory, RAS, Russia

Using available multiwavelength data for the pulsars of different ages detected in the optical range, we analyze the efficiencies of the conversion of the pulsar spindown power  $\dot{E}$  into the observed non-thermal luminosity  $L$  in different spectral domains. We find that these pulsars show significantly non-monotonic dependencies of the optical and X-ray efficiencies ( $\eta = L/\dot{E}$ ) versus pulsar age with a pronounced minimum at the beginning of the middle-age epoch ( $\sim 10^4$  yr) and comparably higher efficiencies of younger and older pulsars. In addition, we find a strong correlation between the optical and 2–10 keV X-ray luminosities of these pulsars that implies the same origin of their nonthermal emission in both spectral domains.

## 1. Introduction

The properties of the observed pulsar emission show that radio and gamma-ray photons have nonthermal origin and are produced by relativistic particles in different parts of the pulsar magnetosphere. The soft X-ray-optical radiation can be a combination of several nonthermal spectral components from the magnetosphere and thermal components from the whole surface of a cooling neutron star (NS) and from its hot polar caps heated by the relativistic particles from the magnetosphere. The nonthermal component has been found to dominate the optical emission of several young, middle-aged, and old pulsars. It is believed that nonthermal components are powered by NS rotational energy loss  $\dot{E} = 4\pi^2 I \dot{P}/P^3$ , where

$I \approx 1.1 \times 10^{45} \text{ gm cm}^2$  is the inertia momentum of a NS of  $1.4 M_\odot$  and 10 km radius,  $P$  and  $\dot{P}$  are the pulsar period and its derivative, respectively.  $\dot{E}$  is frequently called also the spindown luminosity and denoted as  $L_{sd}$ . The ratio  $\eta = L/\dot{E}$ , where  $L$  is the photon luminosity, is used to characterize the efficiency of the conversion of  $\dot{E} \equiv L_{sd}$  into the pulsar emission at a given spectral domain. In this paper, we analyze the evolution of the nonthermal luminosities and efficiencies of pulsars detected in the optical range. Such analysis has been performed about 10 yr ago in pioneering works [1,2]. However, considerable progress in the pulsar distance measurements, and much higher quality of recent optical and X-ray observations allowing to resolve better the nonthermal and thermal emission components from

Table 1

The dynamical ages  $\tau = P/2\dot{P}$ , distances  $d$ , spindown luminosities  $\dot{E}$  (or  $L_{sd}$ ), and observed nonthermal luminosities in the radio,  $L_R$ , optical,  $L_{Opt}$ , X-rays,  $L_X$ , and gamma-rays,  $L_\gamma$ , of seven radio pulsars detected in the optical range [4,5]. Figures in brackets are  $\pm 1\sigma$  uncertainties of the values.

Source	$\log \tau$ [yr]	$d$ [pc]	$\log \dot{E}$ [erg s <sup>-1</sup> ]	$\log L_R^a$ [mJy kpc <sup>2</sup> ] 408 MHz	$\log L_{Opt}$ [erg s <sup>-1</sup> ] B band	$\log L_X$ [erg s <sup>-1</sup> ] 2-10 keV	$\log L_\gamma$ [erg s <sup>-1</sup> ] $\geq 400$ MeV
Crab	3.1	$2.0 \times 10^3$	38.65	3.41(4)	33.23(5)	$36.67^{(+20)}_{(-26)}$	$35.7^{(+1)}_{(-3)}$
B0540-69	3.2	$5.0 \times 10^4$	38.17	3.30(9)	33.47(15)	$36.99^{(+19)}_{(-23)}$	$\leq 35.97$
Vela	4.1	$293^{(+19)}_{(-17)}$	36.84	2.64(20)	28.3(3)	$31.2^{(+36)}_{(-38)}^i$	$33.9^{(+1)}_{(-3)}$
B0656+14	5.0	$288^{(+33)}_{(-27)}$	34.58	-0.27(9)	27.53(8)	$30.30^{(+36)}_{(-28)}$	$32.37^{(+10)}_{(-30)}$
Geminga	5.5	$153^{(+59)}_{(-34)}$	34.51	$0.375^{(+27)}_{(-23)}$	$26.95^{(+16)}_{(-10)}$	$29.35^{(+38)}_{(-36)}$	$32.95^{(+10)}_{(-30)}$
B1929+10	6.5	$361^{+10}_{-8}$	33.59	1.52(5)	$27.26^{(+20)}_{(-33)}$	$29.86^{(+13)}_{(-15)}$	$\leq 32.57$
B0950+08	7.2	262(5)	32.75	1.44(16)	26.88(8)	$29.28^{(+13)}_{(-18)}$	$\leq 32.51$

<sup>a</sup> The radio luminosity is defined traditionally as  $L_R = S_{408} d_1^2$  [mJy kpc<sup>2</sup>], where  $S_{408}$  is the observed flux density from a pulsar at 408 MHz in mJy, and  $d_1$  is its distance in kpc. At a typical radio band FWHM of about 100 kHz the conversion factor to standard luminosity units is  $\approx 9.51 \times 10^{21}$  [erg s<sup>-1</sup>]/[mJy kpc<sup>2</sup>].

the pulsars and to identify in these ranges several new objects enable us to update significantly previous analysis and to get qualitatively new results on the evolution of old pulsars.

## 2. The sample and data sources

We have analyzed multiwavelength non-thermal luminosities of seven pulsars detected in the optical range (see Table 1; [4,5]). The advantage of this sample is a small (<10%) uncertainty in the distances to the pulsars, determined from the radio or optical parallax measurements. This strongly minimizes errors in the inferred luminosities. Distances for a few other

optical pulsars are much less certain and we excluded them from consideration. In the optical we used the data obtained in the B-band [4,5] since practically all the pulsars from our sample were detected in this band and fluxes in other bands are not strongly different from these. Using this band also allows us to escape possible contamination of the pulsar fluxes by strong nebular lines in cases when an associated nebula around a pulsar exists, or is expected to exit. In X-rays we used the data obtained in 2-10 keV range [6,5], where the nonthermal power law spectral tails dominate over the thermal components detected from several pulsars in a

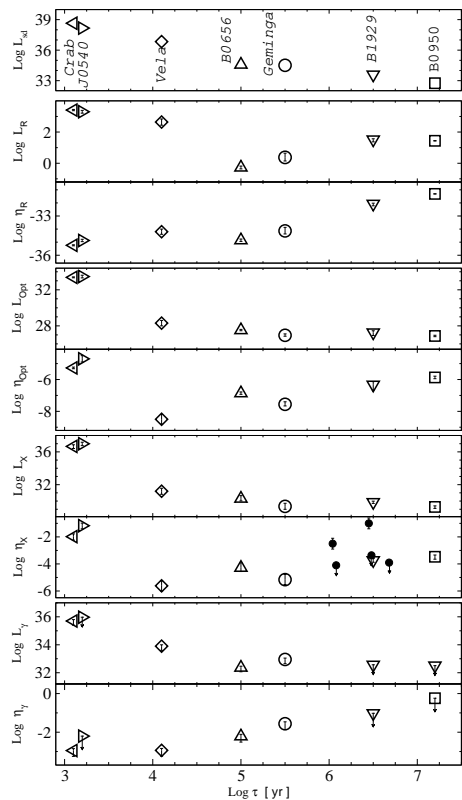


Figure 1. *From top to bottom:* evolution of the pulsar spindown, radio, optical, X-ray, and gamma-ray luminosities and respective efficiencies, with dynamical age. Filled circles are the data taken from [7]. Hereafter errorbars and arrows show  $\pm 1\sigma$  value uncertainties and  $1\sigma$  upper limits, respectively.

softer energy range. We added also the data from [7] on 5 old pulsars recently observed with the Chandra and XMM. In the radio and gamma-rays we used the data obtained at 400 MHz (ATNF catalog [8]) and in the EGRET range of 400 MeV–10 GeV [9], respectively. Here we consider only isotropic equivalents of the luminosities neglecting the emission beaming which is not yet properly known in the all considered ranges for all our objects.

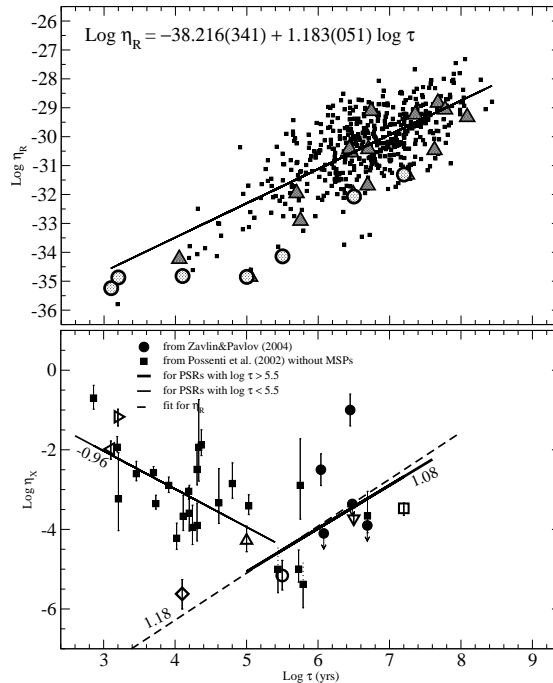


Figure 2. *Top:* radio efficiencies of 500 pulsars from ATNF [8] *vs* dynamical age; triangles mark the pulsars with more accurate parallax-based distances and circles select optical pulsars from Table 1. *Bottom:* X-ray efficiencies *vs* dynamical age; lines are the linear regression fits of evolution tracks of younger and older pulsars and numbers show the line slopes.

### 3. Results

#### 3.1. Evolution

The nonthermal luminosity and efficiency evolution of pulsars in different spectral domains, based on the selected sample of the optical pulsars, is shown in Fig. 1. We note the following points:

(1) the spindown luminosity decreases monotonically with age, as expected from a formal dependence  $\dot{E} \sim \tau^{-1}P^{-2}$  and

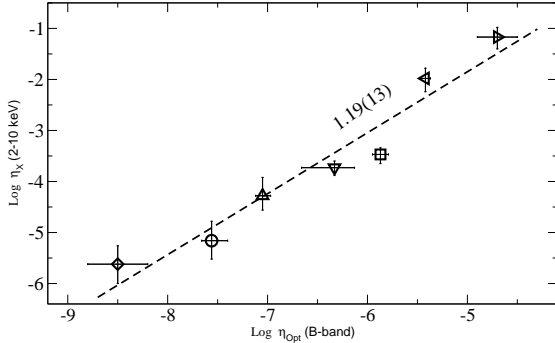


Figure 3. Relationship between the optical and X-ray efficiencies in the B band and 2-10 keV ranges.

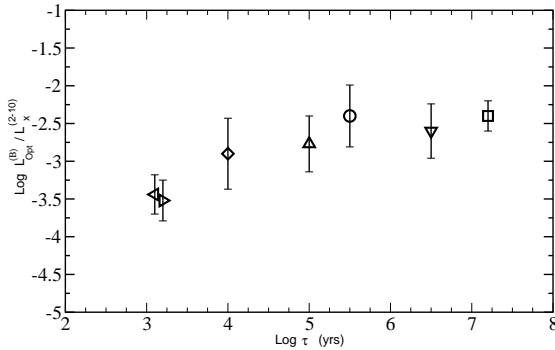


Figure 4. The evolution of the optical and X-ray luminosities ratio with dynamical age.

longer periods of older pulsars; (2) the optical, X-ray and gamma-ray luminosities also decrease with age, but become almost constant starting from a middle-age epoch of  $10^4 - 10^5$  yr; (3) the radio luminosity is less monotonic but starts to increase gradually approximately from the same age; (4) as a result, the evolution of the optical and X-ray efficiencies is non-monotonic and shows a pronounced minimum efficiency at a middle-age epoch of  $10^4 - 10^7$  years and comparable higher efficiencies for younger and older pulsars in contrast to the conception of a mono-

*S. Zharikov, Yu. Shibano, V. Komarova*

tonic decrease of the efficiency with age suggested by [2] through lack of data on old pulsars at that time; (5) the shapes of the dependencies  $\eta_{opt}(\tau)$  and  $\eta_X(\tau)$  are remarkably similar to each other; (6) the radio and gamma-ray efficiencies increase with age but their increases becomes apparently steeper from the same middle-age epoch.

The fact that older pulsars are much more efficient radio emitters than younger ones is confirmed at a much higher significance level based on a rich sample of radio pulsars extracted from the ATNF catalog (Fig. 2, top panel). The scatter of the data along the mean evolution track shown in this panel by solid line may be explained by different geometrical/beaming factors and uncertainties in the distance. The pulsars with parallax based distances are generally below this line. This may reflect a systematic shift between the parallax and dispersion measure distances used for the rest objects.

The nonmonotonic efficiency evolution in X-rays becomes much less obvious if we consider a larger sample of pulsars identified in X-rays including a few of them identified in the optical and X-rays (Fig. 2. low panel). The statistics is much poor than in the radio and this picture is more affected by the distance and flux uncertainties. Nevertheless, applying linear regression fits separately to sub-samples of sub-middle-aged and post-middle-aged pulsars, one can resolve hints of the non-monotonic evolution clearly seen in the optical sub-sample. In the example shown in Fig.2, (low panel) the Geminga age of

$10^{5.5}$  yr, when the optical efficiency start to increase, was used to divide by subsamples. In this case the evolution track of older pulsars may be compatible with what is seen in the radio range (cf. dashed and solid lines). Using other dividing ages from the range of the middle-aged epoch of  $10^4 - 10^6$  yr does not change the picture qualitatively though slopes values can be different, but they are always negative and positive for younger and older pulsars, respectively. In all of the X-ray plots we added X-ray data for 5 old pulsars detected recently with Chandra and XMM [7]. These data are likely to be consistent with the proposed evolution picture. To confirm or reject it better quality X-ray data and distance information are needed.

### 3.2. Correlation between the optical and X-ray emission

Similar shapes of the optical and X-ray evolution tracks suggest a correlation between the luminosities in these domains. This is confirmed by the linear regression fit of the  $\eta_{opt}$  vs  $\eta_X$  distribution shown in Fig. 3. The correlation coefficient is 0.97. A strong correlation implies the same origin for the emission in both spectral domains. It is independent of the difference in the spectral slopes in these ranges observed for the pulsars of different age. For instance, the extrapolation of the non-thermal component of the X-ray spectrum of young Crab-like pulsars strongly overshoots the observed optical fluxes, while for older pulsars the optical fluxes are generally compatible with such extrapolation. This is reflected in the evolution of the ratio  $L_{opt}/L_X$  shown in Fig. 4. The ratio

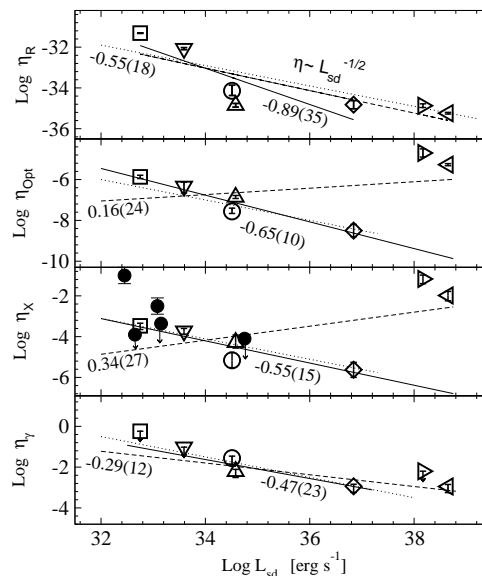


Figure 5. *From top to bottom:* relationships between the efficiencies in the radio, optical, X-ray, and  $\gamma$ -ray spectral domains and spindown luminosity. Different pulsars are denoted by the same symbols, as in Fig. 1. Dashed and solid lines show the best linear regression fits of the whole set of pulsars, and without the two younger ones (Crab and PSR B0540-69, with the highest  $L_{sd}$ ), respectively. The slope values are indicated near the lines. Dotted lines indicate a slope in case of the linear proportionality of the luminosity to the Goldreich-Julian current [3].

becomes almost independent of age starting from a middle-age epoch.

### 3.3. The efficiency and the spindown luminosity

The distributions of the efficiencies of the optical pulsars in different spectral domains vs spindown luminosity are shown in Fig. 5. These distributions demonstrate that: (1) in the radio and gamma-rays,

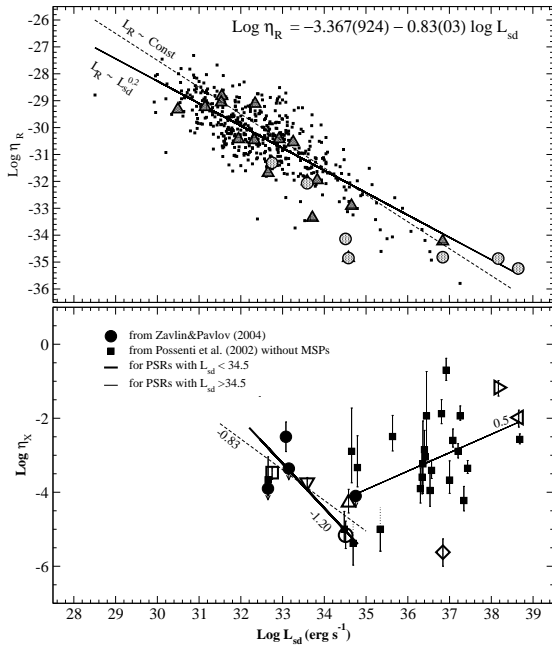


Figure 6. *Top*: radio efficiencies of 500 pulsars from ATNF database [8] vs  $L_{sd}$ ; notations are the same as in Fig. 2. *Bottom*: X-ray efficiencies vs spin-down luminosity; lines fit the distribution of lower and higher  $L_{sd}$  pulsars; numbers show the line slopes.

less energetic pulsars (with low  $L_{sd}$ ) are more efficient photon emitters than more energetic ones; (2) in these ranges the efficiency increases monotonically with the  $L_{sd}$  decrease; (3) the same is seen in the optical and X-ray ranges with an exclusion of the two most energetic and young pulsars, Crab and PSR B0540-69, which form a separate sub-class in these distributions; (4) recent data for the five old pulsars identified in X-rays (filled circles in Fig. 5) do not change the above tendency in X-rays and may even strengthen it (cf. Fig. 6, bottom panel).

As in case of the evolution picture, the fact that the pulsars with lower  $L_{sd}$  are more effective radio emitters is firmly confirmed by the analysis of a much larger sample of pulsars extracted from the ATNF catalog [8] (Fig. 6, top panel). Comparing the triangles and black point distributions in Fig. 6, (top panel), we can note that the scatter around an average distribution shown by the solid line is likely equally caused by uncertainties in the pulsar geometry (triangle points), and DM-based distances (black points). The slope of the distribution is different from a trivial one assuming  $L_R \sim const$  (dashed line in this plot) but suggests an increase of the radio luminosity  $\propto L_{sd}^{0.2}$ .

The separation into two sub-classes of the low and high spindown luminosity pulsars that is clearly seen in the middle panels of Fig. 5 for the optical pulsars is not obvious for a wider sample of pulsars identified in X-rays (Fig. 6, bottom panel). The reasons are likely to be the same as we have mentioned in Sect. 3.2 (poor statistics + distance and flux uncertainties). However, as in the case of the evolution picture for the same sample shown in Fig. 3, linear regression fits allow us to resolve a hint of a bimodal distribution with the efficiency increases toward the low and high sides of the considered  $L_{sd}$  range. The bottom panel of Fig. 6, where  $L_{sd}$  of Geminga was used, as in case of Fig. 3, to divide the pulsars by subsamples, suggests also that the distribution of the low  $L_{sd}$  pulsars may be roughly compatible with what is seen in the radio range (cf. solid and dashed lines in this

plot). The suggested bimodal distribution can hardly be explained by geometry effects, if we compare the relatively small scattering of the triangle points around a mean distribution in the radio (top panel), likely caused by geometry effects, and the much larger scattering of all points in X-rays (bottom panel).

#### 4. Summary

Our multiwavelength analysis of the nonthermal luminosity and efficiency distributions *vs* dynamical age and spin-down power of the pulsars detected in the optical range suggests significantly non-monotonic evolution of their emission in the optical and X-ray domains and/or a bimodal distribution of the respective efficiencies *vs* spindown power. Less energetic old pulsars are much more efficient photon emitters than the middle-aged ones and their efficiency is comparable with that for the much younger and energetic Crab-like objects. The bimodal structure is not significant but still resolved in a larger sample of pulsars identified in X-rays, where it may be smoothed by large distance and flux uncertainties and needs further study. An apparent evolution track of old pulsars in the optical and X-rays is roughly compatible with the track seen in the radio range where the evolution is accompanied by a significant increase of the radio-efficiency with NS age. If it is true, this implies an universal engine that drives the non-thermal evolution of old pulsars by a unified way increasing their efficiency with age in the all spectral domains.

This work has been partially supported by CONACYT project 36585-E, and RFBR grants 02-02-17668, 03-02-17423, 03-07-90200 and RLSS 1115.2003.2

#### REFERENCES

1. Mereghetti, S.; Caraveo, P. A.; Big-nami, G., Multiwavelength observations of isolated neutron stars, *ApJS* 92, 521-526, 1994
2. Goldoni P., Musso, C., Caraveo, P. A., et al., Multiwavelength phenomenology of isolated neutron stars, *A&A*, 298, 535-543, 1995
3. Goldreich, P., Julian, W. H., Pulsar electrodynamics. 157, 869-880, 1996
4. Zharikov, S. , Shibano, Yu., Koptsevich, A., et al., Subaru optical observations of the old pulsar PSR B0950+08, *A&A*, 394, 633-639, 2002
5. Zharikov, S., Shibano, Yu., Mennickent, R., et al., Multiband optical observations of the old PSR B0950+08, *A&A*, 417, 1017-1030, 2004
6. Possenti, A., Cerutti, R., Colpi, M., et al., Re-examining the X-ray versus spin-down luminosity correlation of rotation powered pulsars, *A&A*, 387, 993-1002, 2002
7. Zavlin V., Pavlov G., X-ray emission from the old pulsar B0950+08, *ApJ*, 616, 452-462 2004
8. [www.atnf.csiro.au/research/pulsar](http://www.atnf.csiro.au/research/pulsar)
9. Thompson, D., High Energy Emission from Active Pulsar, *AdSpR*, 25, 659-668, 2000